Comparative study of tripropylamine and naphthylamine as additives in wave solder flux: investigation of solderability and corrosion effects

Feng Li[1,*] , Morten Stendahl Jellesen[1], and Rajan Ambat[1]

[1] *Section of Materials and Surface Engineering, Department of Mechanical Engineering, Technical University of Denmark, 2800 Kgs. Lyngby, Denmark*

ABSTRACT

Dicarboxylic acid flux activators are used in no-clean wave solder flux formulation for activating the solder surfaces on Printed Board Assembly (PBA) during the soldering process. However, flux residues containing dicarboxylic acid chemistry on PBA can cause adverse corrosion issues under humid conditions due to its hygroscopic and acidic nature. This paper systematically investigated tripropylamine and naphthylamine as additives together with dicarboxylic acid activators on the solderability performance and humidity robustness. Evaluation of the solderability was assessed using hot plate spreading test and wetting balance methods, while thermal degradation was investigated using Fourier-transform infrared spectroscopy. The moisture interaction behavior of activator chemistry was investigated using electrochemical impedance spectroscopy and chronoamperometry techniques. Results showed improvement of wetting ability using tripropylamine additive in succinic acid based fluxes, while tripropylamine additive increased the maximum wetting force for adipic acid based flux activators. Significant reduction of leakage current value was obtained using tripropylamine and naphthylamine additives in succinic acid based fluxes under 98% RH/40 °C.

1 Introduction

Due to the green manufacturing trends in the electronic industry, halogenated cleaning solvents for printed board assembly (PBA) and leaded solders were phased out based on Montreal Protocol [1] and Waste Electrical and Electronic Equipment (WEEE) [2] directives. Hence, elimination of cleaning steps in electronic manufacturing became the trend in order to decrease the utility of the volatile organic cleaning agents [3, 4]. Consequently, no-clean flux formulation was broadly implemented over 70% of the electronic industry [5, 6]. The role of no-clean solder flux system is to remove the oxide on the metal bonding surface [7] and prevent re-oxidation of the molten solder alloys [8, 9], while leaving a minimal flux residue due

Address correspondence to E-mail: feli@mek.dtu.dk

to thermal evaporation or degradation during soldering process [10, 11]. No-clean flux for wave soldering process used today contains activators, non-polar vehicles, solvents, surfactants and other organic additives [7, 12, 13]. Compared to other chemical constituents in no-clean flux formulation, weak organic acid (WOA) activators was identified as the most deteriorate chemical content from corrosion reliability point of view [11, 14, 15]. Commercially used WOA based flux systems today use activators such as adipic acid, succinic acid, glutaric acid, stearic acid etc. [4, 6, 16, 17], which possess boiling temperature at 337.5 °C, 234 °C and 273 °C respectively [18]. In practice, the soldering temperature is usually set between 230 and 250 °C to avoid the damage of components on PBA [19, 20]. Even though the soldering temperature may degrade succinic acid and form degradation product (succinic anhydride), the degradation product will present on PBA due to the higher boiling point [4]. Therefore, significant amount of WOA contained flux residue was detected in many electronic devices after soldering process [21–24], and the localized contamination level of WOA can be as high as 687 μg/in^2 (106.5 μg/cm^2) [23].

A number of investigations reported that the WOA contained flux residue on PBA surface can trigger corrosion related failures such as reduction of the surface insulation resistance (SIR) [10, 25, 26], parasitic leakage issue under low stand-off components [23], and electrochemical migration (ECM) [27, 28]. ECM is one of the most detrimental failure mode for the electronic corrosion, and the failure rate of ECM in electronic devices can be as high as 1–4% [29]. For a PBA under exposure to humidity, corrosion cell forms when water layer condensed between oppositely biased electrodes. Bias on the electrodes and the electrochemical process, trigger metal dissolution at the anode, which migrate towards the cathode and deposit forming conductor bridge and short circuit [30, 31]. Under humidity exposure, the hygroscopic behavior of WOA activators in the flux residue changes the humidity level for condensed water layer formation, due to the difference in the critical relative humidity (cRH) [32, 33]. Acidity and ionization behavior of WOA also reduced the pH of the condensed water layer and increased conductivity, while both of these aspects will favor ECM dendrite formation [34]. The solderability and corrosivity of WOA activators depend on the acid dissociation constant (pKa), which is affected by the polarity of the WOA. The PBA contaminated by WOA with shorter carbon chain (such as glutaric acid) is more aggressive for ECM [35], although the glutaric acid provides better solderability [36]. Glutaric acid also has lower cRH leading to water layer formation on PBA under lower humidity level when exposed to humidity.

In order to balance the corrosion effect and solderability of the no-clean flux, blended WOA activators [35], blended WOA-amine activators [15, 37], and corrosion inhibitors [15] were introduced to the flux formulation. Piotrowska et al. reported the binary blended WOAs as activators resulting in a lower cRH than the individual WOA, which indicates the water condensation and corrosion can occur at even lower RH value [14] if the level of WOAs are not optimized. Tolla et al. reported the inhibition of ECM dendrite growth obtained by blended anonymous organic amine and WOA, and corrosion inhibitor used in the study was not as good as organic amine candidates [15]. Xu et al. reported that the blended WOA and triethanolamine (TEA) exhibited better solderability and minor corrosion by Cu mirror test [38]; however, in the study, low deliquescence RH of TEA (below 30% RH) was attributed to humidity interaction with hydroxyl group of TEA, which induced ECM dendrites formation under 5 V DC load at 70% RH/25 °C [36]. The humidity robustness of the organic amine activator candidates in flux formulation also depend on the protonation strength of the lone pair in amino group, which could induce the water dissociation for the formation of negatively charged hydroxide ions [39]. The protonation behavior of amine activator residues could be influenced by the environmental temperature, for example, the protonation of diethanolamine (DEA), TEA and triisopropanolamine (TIPA) was significantly prohibited by increasing testing temperature from 25 to 60 °C [36]. Moreover, strong water absorption behavior was obtained by alkanolamine due to the intermolecular hydrogen bond formation between hydroxyl group in alkanolamine and hydrogen in the water molecule from air, which accelerated the ECM failure in electronics [36]. Therefore, it is important to understand the behavior other amine categories such as aromatic amine and alkyl-amine types on their performance of solderability and humdity related corrosion effects.

Tripropylamine and naphthyamine were tested in the present investigation as the representative materials for alkyl-amine and aromatic amine. The present study systematically investigated the amine additives in WOA activator based flux formulation on the solderability and corrosion reliability. SIR comb structure pattern (IPC-4201/21) was used as vehicle for electrochemical tests. Chronoamperometry was used to investigate the leakage current level and ECM susceptibility induced by the flux residue. Electrochemical impedance spectroscopy (EIS) was used to understand the critical relative humidity for model flux with/without organic amine additives. The solderability of organic amine modified flux formulation was investigated using wetting balance. The degradation product of flux residue was analyzed using fourier-transform infrared spectroscopy (FT-IR).

2 Materials and experimental methods

2.1 Materials preparation

2.1.1 Model flux formulation used in the investigation

Table 1 shows physical and chemical properties of two organic amines and two WOAs used for the investigations. All chemicals used are in analytical grade (Sigma Aldrich, USA). The melting point indicates the temperature at which the chemical become liquid and protected the soldering region from re-oxidation. Due to the low melting point of tripropylamine at − 93.5 °C, it presents as liquid state at room temperature. Naphthylamine, succinic acid, and adipic acid require higher temperatures to melt. The boiling point demonstrates the temperature for the evaporation of chemicals, which directly influence the soldering function. The acidic dissociation constant (pKa) determines the solubility of chemicals in water and the strength for the oxides dissolution during soldering condition. Low pKa value of chemicals indicates higher acidity. Table 2 shows the flux formulation and the codename of the model fluxes used in the investigation. The fraction of the WOA activators was maintained at 4 wt%, whereas organic amine additives were set at 0.2 wt% and 0.4 wt%. The flux activator and amine additive was dissolved in insopropanol alcohol by 30 min by ultrasonic bath mixing.

2.1.2 Cu alloy substrates for solderability analysis

For the wetting balance tests (IPC-TM-650 2.4.14.2), the ETP grade Cu substrates with dimension of 6 mm × 25 mm × 0.5 mm were prepared using electronic discharge machining. For the hot plate spreading tests (IPC-TM-650 2.4.46), Cu63/Zn37 brass substrates with dimension of 40 mm × 75 mm × 1 mm were prepared. Cleaning of the test substrate was carried out based on ISO 9455–16 standard.

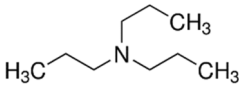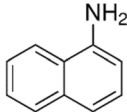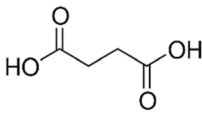**Table 1** Properties of the WOAs and organic amines used in the investigation
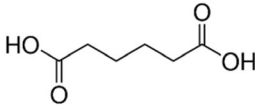
	Molecular structure	Molecular weight(g/mol)	Melting point (°C)	Boiling Point (°C)	pKa1	pKa2
Tripropylamine		143.27	-93.5	156	10.65	–
Naphthylamine		143.18	49.2	300.8	3.92	–
Succinic acid		118.09	188	235	4.21	5.64
Adipic acid		146.14	153.2	337.5	4.43	5.41

Table 2 Model flux formulation used in the investigation

Model flux	Model flux formulation (Solvent: isopropanol alcohol)
A	4 wt% Adipic acid
S	4 wt% Succinic acid
AT02	4 wt% Adipic acid, 0.2 wt% Tripropylamine
AT04	4 wt% Adipic acid, 0.4 wt% Tripropylamine
AN02	4 wt% Adipic acid, 0.2 wt% Naphthylamine
AN04	4 wt% Adipic acid, 0.4 wt% Naphthylamine
ST02	4 wt% Succinic acid, 0.2 wt% Tripropylamine
ST04	4 wt% Succinic acid, 0.4 wt% Tripropylamine
SN02	4 wt% Succinic acid, 0.2 wt% Naphthylamine
SN04	4 wt% Succinic acid, 0.4 wt% Naphthylamine

2.1.3 Test vehicle for corrosion evaluation using electrochemical methods

Test boards (IPC-4201/21) with SIR comb pattern was used for the electrochemical study, as shown in Fig. 1. The surface finish of the SIR pattern was using hot air solder leveled (HASL) Sn-0.7Cu alloy on 35 μm Cu trace. In the total testing area of 25 mm × 13 mm, the entire overlapping length of conductive lines is 442.8 mm with 41 adjacent sets of electrodes. The pitch size of the conductive lines is 300 μm. The cleaned HASL comb structure SIR board used in this work obtained reproducible leakage current of 1 nA under 25 °C/98% RH, which could transfer to 1 GΩ for each 1 V of operation voltage. Before subjecting the electrochemical tests, the testing region of SIR pattern was contaminated to the level of 100 μg/cm² simulated flux residue to imitate the localized contamination after soldering process. Amount of flux applied was simulating the flux applied during actual soldering application. Due to the limitation of the experimental condition, thermal profile of wave soldering is not able to precisely obtained. In order to adapt the peak temperature of 235–260 °C for 10 s

following by a cooling rate of 2–5 °C/s for PBA in actual wave soldering bath [40–42], the thermal effect of the soldering process on flux residue was simulated using a Techno HA-06 oven for a thermal treatment at 240 °C for 45 s. Flux activator contaminated SIR comb patterns without subjecting to thermal exposure were used as reference for the electrochemical tests.

2.2 Solderability evaluation using hot plate spreading testing and wetting balance

2.2.1 Hot plate spreading test

Hot plate spreading tests were conducted using two SD160 digital hotplates (Stuart, UK). An O-ring in diameter of 1 cm was prepared using flux-free 96.5Sn–3Ag–0.5Cu (SAC 305) solder alloy. Before testing, 50 μL of the model flux was applied in the center of the solder O-ring on the Cu63/Zn37 substrate. After 4 s preheat treatment at 160 °C, the sample was subjected on the other hot plate with a temperature of 270 °C until the solder O-ring melted. The spreading of the melted solder alloy was visualized using a light optical microscope (LOM) (Keyence VHX, Japan).

2.2.2 Wetting balance test

Investigation of the solderability of the model fluxes was carried out using the Must 3 wetting balance (GEN3, UK) at an air-static environment, which provided the wetting force of the SAC 305 solder alloy on the flux activated Cu substrates during wave soldering process. To apply the flux, the tested side of cleaned Cu substrate was vertically immersed in the model flux to a depth of 10 mm and cleaned the extra
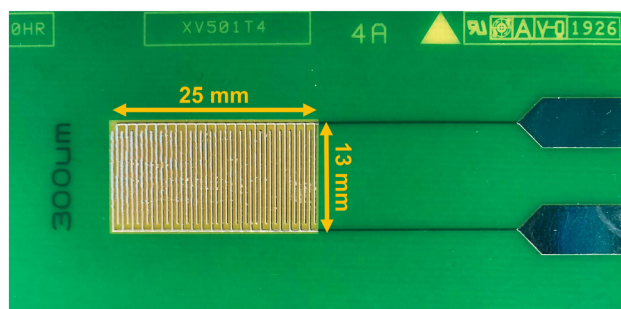

Fig. 1 Test boards with SIR comb structure pattern used for electrochemical study

flux using a filter paper as described in the procedure of IPC-TM 650 2.4.14.2. The temperature of SAC 305 solder bath in the wetting balance was precisely controlled at 270 °C, which provides the heat source for the preheat treatment of Cu samples. After 20 s preheat treatment of the Cu substrate by placing on the solder bath with the distance of 10 mm, the tested side of Cu substrate was immersed in the solder bath for 10 s with the immersion depth of 5 mm in the speed of 20 mm/s. After soldering process, the quality of interface between the SAC 305 alloy layer and the Cu substrate was evaluated by the cross section inspection using the Quanta 200 FEG scanning electron microscope (FEI, USA) under secondary electron mode at 15 kV.

2.3 Thermal decomposition analysis of model flux activators using FT-IR

In order to obtain the structural elucidation of flux activators after soldering process, spectroscopic analysis was carried out using the Nicolet iN10 MX infrared imaging microscope (Thermo Fisher Scientific, USA) equipped with a Ge attenuated total reflectance (ATR) tip. Model flux were placed on the glass substrate and dried in the fume hood, which only leaves the flux activators on the glass substrate. The thermal treatment was carried out on this by placing it in the Techno HA-06 oven at 240 °C for 100 s to simulate the thermal input on flux activators during wave soldering condition. Flux activators without subjecting to thermal exposure was used as reference for the FT-IR analysis.

2.4 Corrosion effects of flux activators using electrochemical techniques

Climatic exposure of the flux activator contaminated SIR comb pattern was conducted in the Espec PL-3KPH climatic chamber (Espec, Japan) with a certainty of ± 0.3 °C and ± 2.5% relative humidity (RH). Electrochemical tests on the SIR comb pattern were performed using the multi-channel Biologic VSP potentiostat (Biologic, France). Three-electrode electrochemical system were used to imitate positive and negative bias on the surface of the PBA. One electrode of the SIR comb pattern was used as counter and reference electrodes, while the other electrode was used as working electrode. Electrochemical tests were conducted at testing temperature

of 25 °C, 40 °C and 60 °C in order to imitate different service condition of electronic device. For instance, 25 °C and 40 °C were used to imitate the environmental temperature, while 60 °C was used to imitate the self-heating of the devices.

2.4.1 Single frequency EIS measurement

Single frequency EIS technique was used to investigate the level of relative humidity (RH) triggering moisture absorption and moisture release from the flux residue contaminated SIR pattern, which will form the basis for corrosion. Moisture absorption of the flux activator contaminated SIR pattern was determined by deliquescence relative humidity (DRH) of the flux activator package, while the moisture release behavior was determined by efflorescence relative humidity (ERH). During water condensation on the PBA, the phase angle of SIR components shifted from − 90° to 0° at high frequency range between 10 and 100 kHz [43, 44], which indicates the transition of electrical property from capacitance dominant behavior to resistance dominant behavior [44]. Consequently, the EIS measurement at such frequency is able to roughly estimate the DRH and ERH [14, 32, 45]. Single frequency EIS at 10 kHz with the amplitude of 10 mV was applied on the flux activator contaminated SIR pattern in order to record the DRH value of flux activator during humidity ramping from 30% RH to 99% RH in 12 h. The ERH value was measured during humidity ramping from 99% RH to 30% RH in next 12 h. Before subjecting the single frequency EIS measurement, flux activator contaminated SIR patterns were stabilized at 30% RH in climatic chamber for 6 h.

2.4.2 Chronoamperometry (CA) testing

CA technique was used to investigate the leakage current or ECM triggering capacity of flux activator contaminated SIR pattern under different humidity exposure conditions namely at 60% RH, 70% RH, 80% RH, 90% RH and 98% RH respectively. Before conducting the CA measurement, the flux activator contaminated SIR pattern was stabilized in the climatic chamber for 1 h. The CA measurement for each type of flux activator contaminated SIR pattern was conducted under 10 V DC bias loads for 3 h. Leakage current level of flux activator contaminated SIR pattern was recorded by EC-lab software. The threshold

value of leakage current value was defined at 1–10 µA based on the previous observation of ECM dendrites formation using IPC-4201/21 SIR comb pattern [35, 45].

3 Results

3.1 Evaluation of etching ability of model fluxes for activation

Figure 2 shows the spreading of the SAC 305 alloy when using different model fluxes after hot plate spreading test. Figure 2 a2–3, b2–3 shows the tripropylamine additive in adipic acid and succinic acid contained model fluxes increased the spreading area of the SAC 305 alloy compared to pure adipic acid and succinic model flux etched sample shown in Fig. 2a1, b1. Figure 2 a5, b5 indicate that the spreading area of SAC 305 alloy decreased using 0.4 wt% naphthylamine additive in activator package. Figure 2a2, a3 shows the tripropylaninе addtive in adipic acid flux expanded the spreading area towards center of the O-ring, however, for the for

tripropylamine modified succinic acid fluxes, spreading tendency was in opposite as shown in Fig. 2b2, b3.

Figure 3 shows the curves of wetting force induced by the model fluxes during wetting balance testing. Time to reach zero wetting force (T_0), time to two thirds maximum wetting force ($T_{2/3}$), and maximum wetting force (F_{max}) were summarized in Table 3. T_0 and $T_{2/3}$ parameters demonstrate the speed of wetting, while the F_{max} parameter demonstrates the solderability. The effect of amine additives on F_{max} was more pronounced on adipic acid contained flux formulations, as shown in Fig. 3a. Compared to 3.69 mN obtained by pure adipic acid model flux (Fig. 3b), the F_{max} was improved using ST02, ST04 and SN02 model fluxes, which were 4.11 mN, 4.08 mN and 3.92 mN respectively. However, the F_{max} of AN04 model flux decreased to the level of 3.49 mN. In comparison, the F_{max} was slightly reduced when using amine additive in succinic acid contained flux formulation. The SN02 and SN04 model fluxes induced slightly lower F_{max} at 3.73 mN compared to ST02 model flux at 3.98 mN and ST04 model flux at 3.89 mN. Generally, the wetting speed of 4 amine additive modified succinic acid model
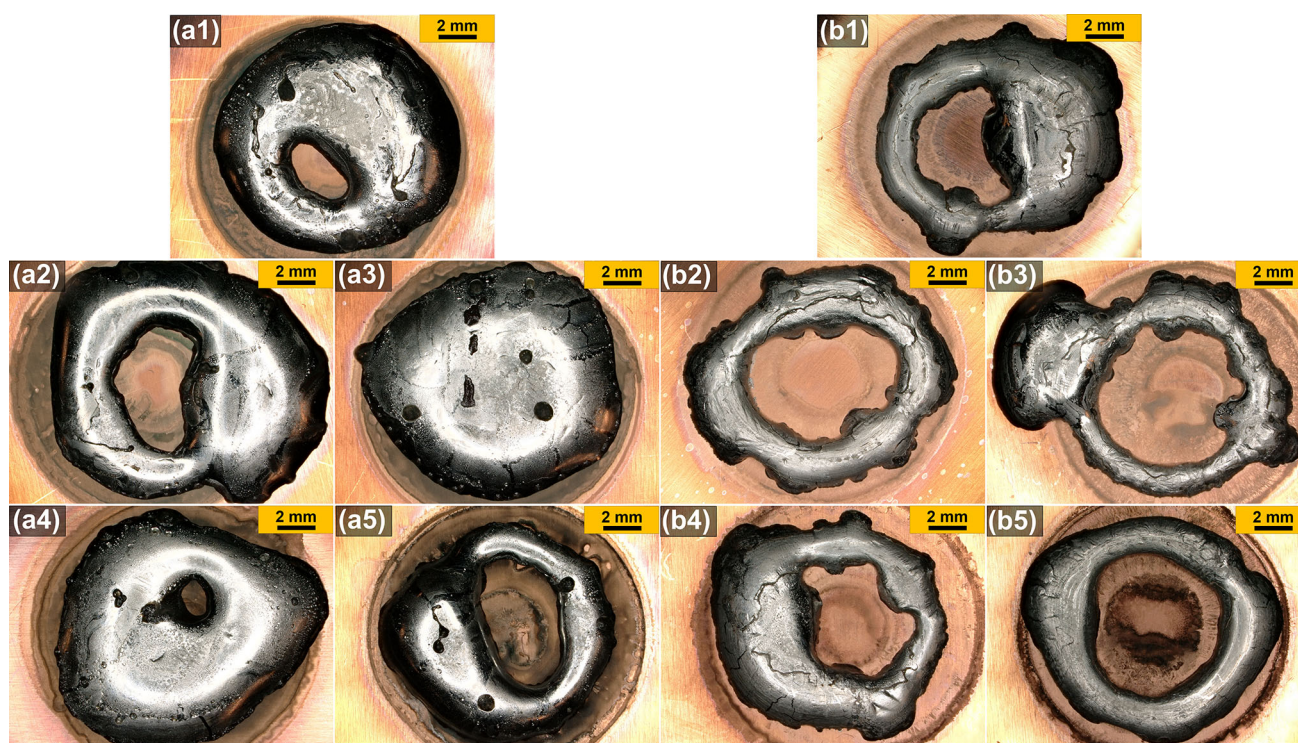

Fig. 2 LOM photographs of specimens after hot plate spreading test using various model fluxes: **a1** A, **a2** AT02, **a3** AT04, **a4** AN02, **a5** AN04, **b1** S, **b2** ST02, **b3** ST04, **b4** SN02, **b5** SN04
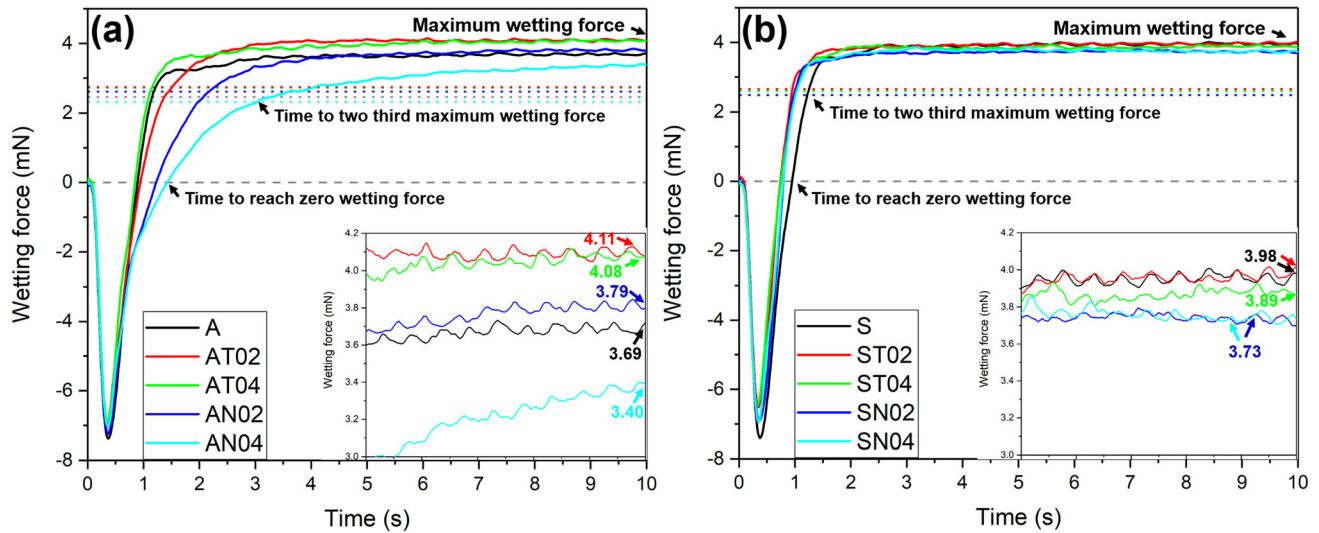
Fig. 3 Wetting balance test result using various model fluxes for surface activation: **a** model fluxes with adipic acid as main activators, **b** model fluxes with succinic acid as main activators

Table 3 Summary of qualification parameters in wetting balance result from 3 parallel tests

	Time to reach zero wetting force (s)	Time to two thirds maximum wetting force (s)	Maximum wetting force (mN)
Adipic acid	0.94 ± 0.09	1.32 ± 0.23	3.69 ± 0.03
AT02	0.97 ± 0.06	1.55 ± 0.06	4.11 ± 0.02
AT04	0.89 ± 0.05	1.18 ± 0.03	4.08 ± 0.03
AN02	1.18 ± 0.05	2.18 ± 0.06	3.92 ± 0.04
AN04	1.38 ± 0.04	2.77 ± 0.20	3.49 ± 0.10
Succinic acid	1.00 ± 0.06	1.34 ± 0.08	3.97 ± 0.04
ST02	0.74 ± 0.03	0.96 ± 0.02	3.98 ± 0.03
ST04	0.75 ± 0.02	1.01 ± 0.02	3.89 ± 0.02
SN02	0.79 ± 0.03	0.99 ± 0.02	3.73 ± 0.03
SN04	0.79 ± 0.01	1.00 ± 0.02	3.73 ± 0.03

fluxes was faster than 4 amine additive modified adipic acid model fluxes. Figure 3a illustrates the wetting speed for adipic contained model flux was significantly influenced by amine additives. The $T_{2/3}$ of AT04 model flux decreased to 1.18 s in comparison with pure adipic acid model flux for 1.32 s, whereas larger T_0 and $T_{2/3}$ were obtained when using AT02, AN02 and AN04 model fluxes, as shown in Table 3. In contrast, the amine additives in succunic acid fluxes reduced the T_0 to approximate 0.74–0.79 s, and the $T_{2/3}$ values for amine additive modified succinic acid model flux were approximate 0.96–1.01 s.

Figure 4 shows the cross-section of the wetting balance tested samples indicating the quality of SAC 305 layer on Cu substrates when various fluxes are used. Some defect was observed on the tip of Cu

substrate activated using pure adipic acid model flux, as shown in Fig. 4a1, while Fig. 4a2–a5 shows perfect coverage of SAC 305 layer was observed when using tripropylamine and naphtylamine modified model fluxes for the test, although the thickness of the SAC 305 layer was different. Compared to pure adipic acid model flux activated sample in Fig. 4a1, a5, a4 shows that the 0.4 wt% and 0.2 wt% naphthylamine additive in adipic acid contained model flux reduced the maximum thickness of the SAC 305 layer from 41 to 38 μm and 28 μm respectively. However, Fig. 4a3 indicates that the maximum thickness of SAC 305 layer in AT04 sample was slightly higher than pure adipic acid model flux activated Cu sample. For the model fluxes with succinic acid as activators, the 0.4 wt% and 0.2 wt% naphthylamine additive
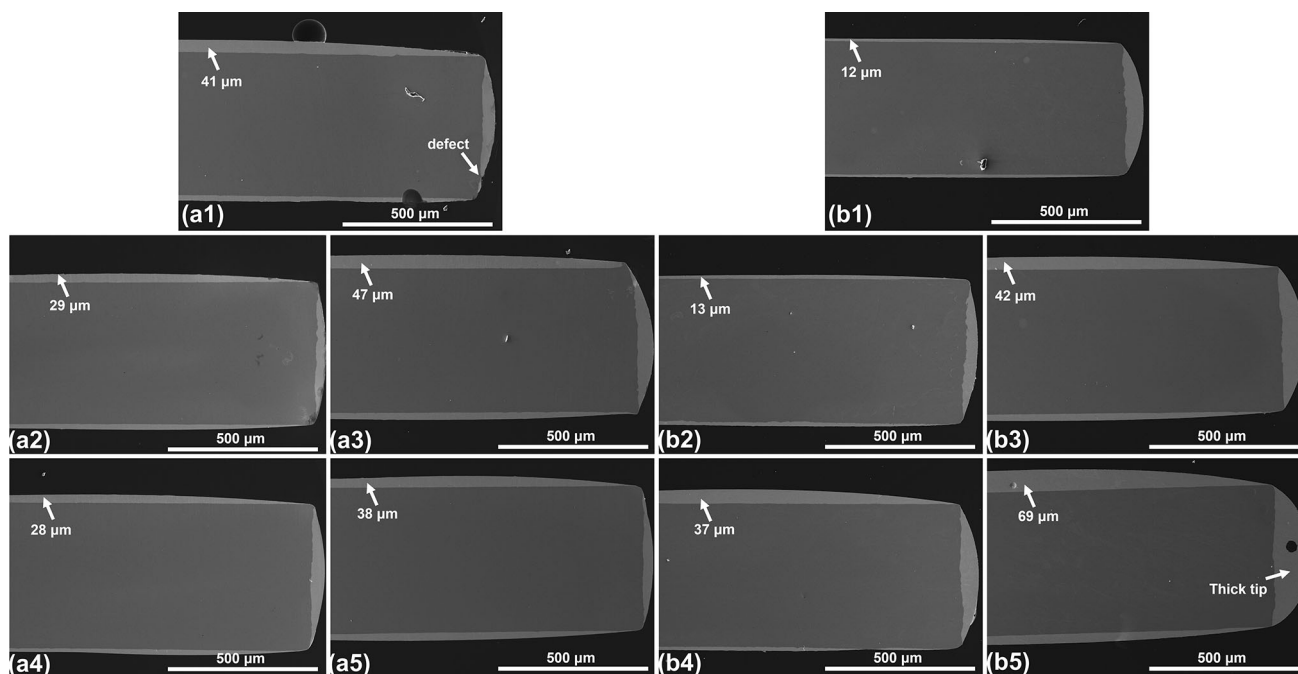
Fig. 4 Secondary electron micrograph of the SAC 305 coated Cu substrates in the view of cross section after wetting balance testing: **a1** A, **a2** AT02, **a3** AT04, **a4** AN02, **a5** AN04, **b1** S, **b2** ST02, **b3** ST04, **b4** SN02, **b5** SN04

increased the maximum thickness of SAC 305 layer from 12 to 69 μm and 37 μm respectively, as shown in Fig. 4b1, b5, b4. Higher maximum thickness of SAC 305 layer at 42 μm was obtained using ST04 model flux in comparison with 13 μm SAC 305 layer using ST02 model flux.

3.2 Evaluation of structural degradation of flux activator packages after thermal activation

Figure 5 illustrates the effect of simulated soldering temperature on the thermal degradation of the tested flux activator packages. Generally, the amide formation was detected in model fluxes with succinic acid activators as shown in Fig. 5c; while none of the amide peak was detected in the model fluxes with adipic acid as activators as shown in Fig. 5a. After adding amine additive in model flux with succinic acid activator as shown in Fig. 5c, the C=O bond at 1685 cm^{-1} split into two peaks which located at 1685 cm^{-1} and 1725 cm^{-1}. The C=O stretching bond at 1685 cm^{-1} belongs to carboxylic acid, while the C=O stretching peak at 1725 cm^{-1} belongs to the newly formed amide. The peak of C–N stretching bond in amide group was detected at 1106 cm^{-1}. Figure 5d shows the degradation of the amide in the

model flux with succinic acid activator occurred after thermal activation at 240 °C. The carboxylic acid C=O stretching bond still presented at 1685 cm^{-1} for pure succinic acid model flux. In the amine additive contained succinic acid fluxes, the amide C=O stretching bond at 1725 cm^{-1} disappeared and the peak of carboxylic C=O stretching bond shifted to left in a range between 1692 and 1696 cm^{-1}. After thermal activation, no significant difference was observed in the spectra of adipic acid based model fluxes in comparison with the non-thermal activated one, as shown in Fig. 5a, b.

3.3 Corrosion investigation of model fluxes

3.3.1 Corrosion assessment due to deliquescence of model fluxes using single frequency EIS

Figure 6 demonstrates the impedance response of model fluxes contaminated SIR patterns due to water film formation on the SIR comb pattern depending on the deliquescence behavior of the model flux. Large impedance drop indicates the detrimental corrosion effects of the flux residue under DC conditions. In general, the reduction of DRH was obtained for all tested model flux activators when increasing the testing temperature from 25 to 60 °C. Under testing

Fig. 5 The FT-IR spectra of tested flux activators with/without thermal treatment: **a** adipic acid contained activator packages with no thermal activation, **b** adipic acid contained activator packages after thermal treatment at 240 °C for 100 s, **c** succinic acid contained activator packages with no thermal activation, **d** succinic acid contained activator packages after thermal treatment at 240 °C for 100 s
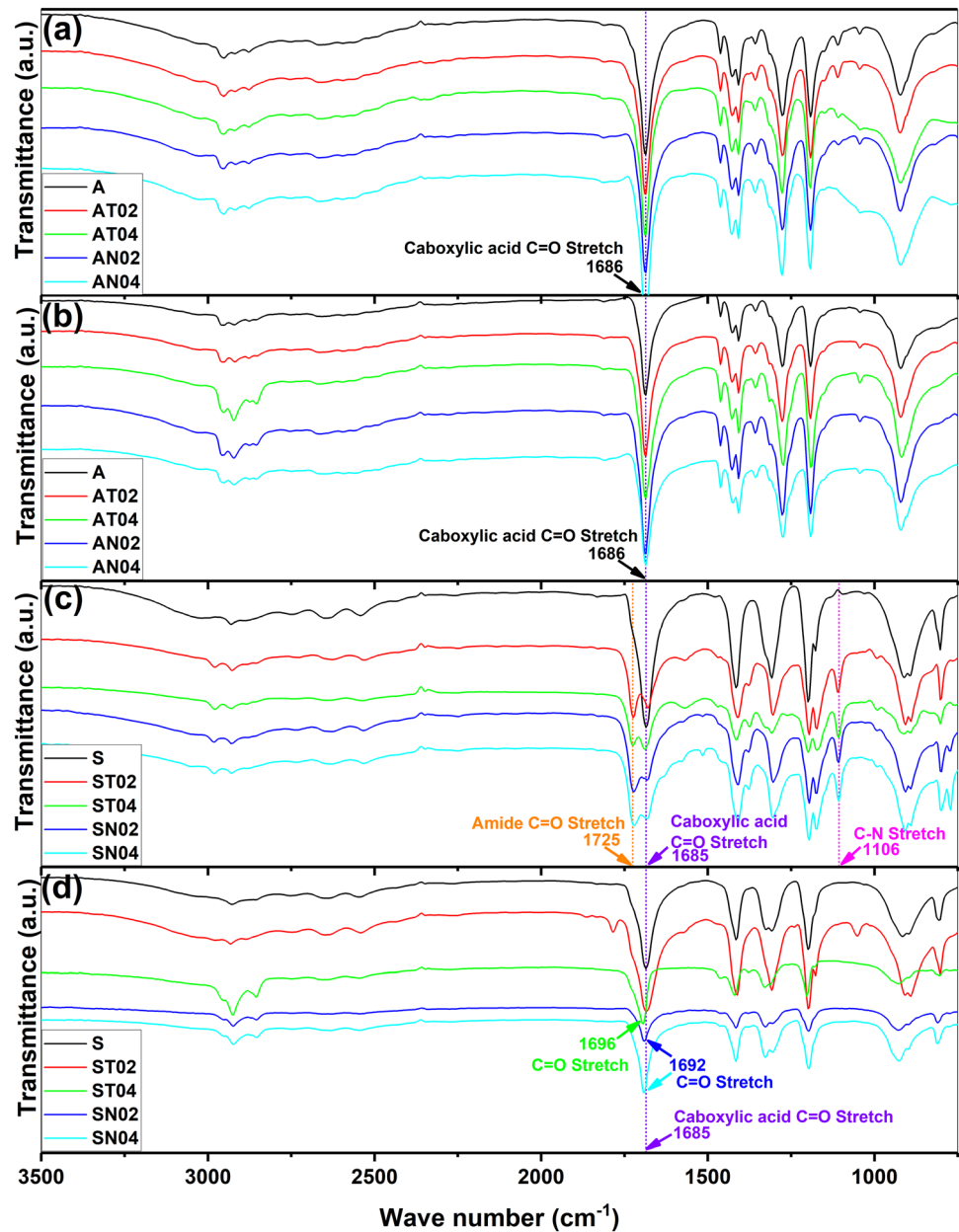
temperature of 25 °C, DRH value of all the tested activator package was beyond 95% RH, and impedance response at 99% RH for all the activator packages was maintained above 500 kΩ. Under testing temperature of 40 °C, significant drop of impedance was obtained by non-thermal activated pure succinic acid contaminated SIR pattern as shown in Fig. 6c2. In contrast, the non-thermal activated amine additive contained succinic acid fluxes exhibited high impedance level above 450 kΩ under 99% RH. After thermal activation at 240 °C (Fig. 6d2), the high level of impedance was obtained again by pure succinic

acid activator contaminated SIR pattern under 99% RH. Figure 6a3, b3, c3, d3 shows that the DRH values of pure adipic acid and pure succinic acid fluxes are within 87–88% RH under the testing temperature of 60 °C, which were higher than ERH value obtained between 67 and 70% RH. In the non-thermal activated adipic acid contained model fluxes shown In Figure 6a3, amine additives slightly improved the DRH and ERH value of activator packages to 90% RH and 84% RH respectively. Compared to the pure adipic acid sample, amine additives significantly improved the impedance response of adipic acid
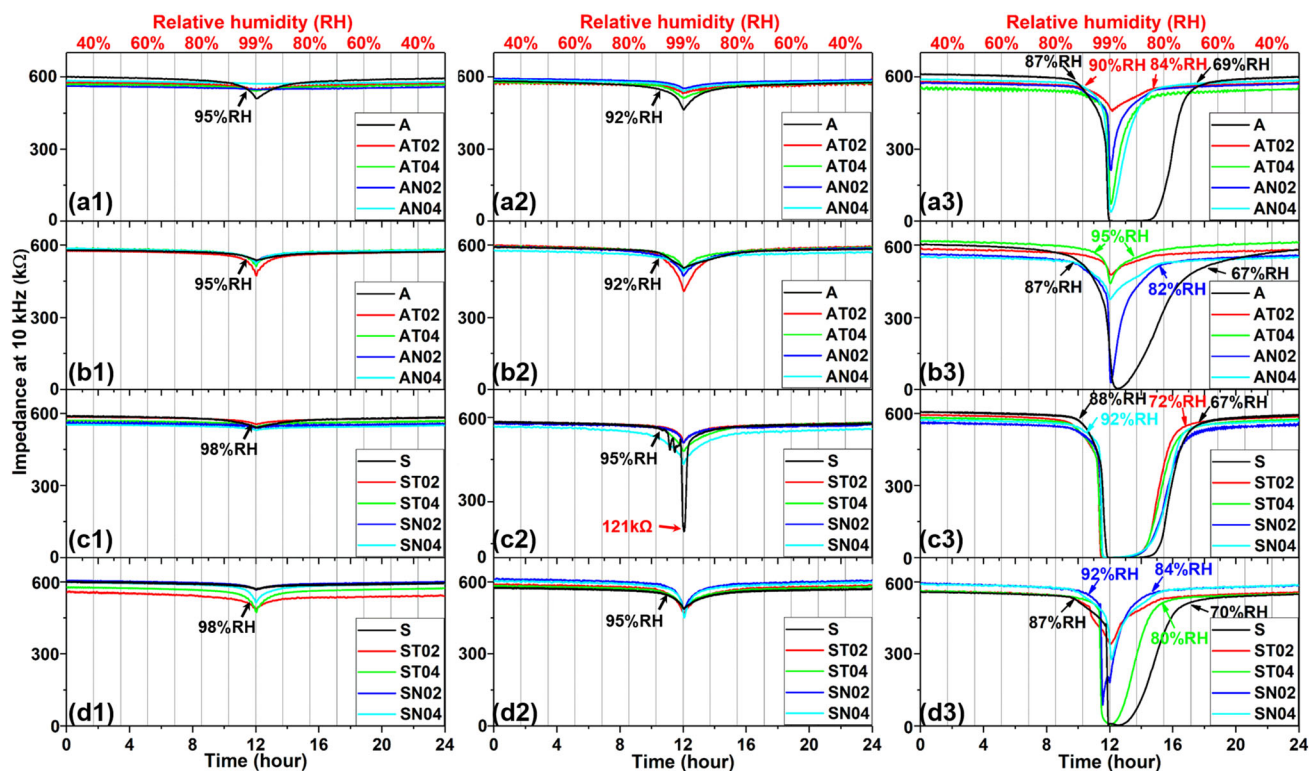
Fig. 6 Impedance response at 10 kHz of SIR pattern contaminated with: **a** non-thermal activated adipic acid model fluxes, **b** 240 °C activated adipic acid model fluxes, **c** non-thermal activated succinic acid model fluxes, **d** 240 °C activated succinic acid model fluxes; under testing temperature of (1) 25 °C, (2) 40 °C, (3) 60 °C

fluxes at 99% RH. However, amine additives did not influence the impedance response of the non-thermal activated succinic acid fluxes under 99% RH exposure, as shown in Fig. 6c3. Under testing temperature of 60 °C, significant improvement of the ERH value and the impedance response at 99% RH was obtained by fluxes with amine additives after thermal activation at 240 °C, as shown in Fig. 6 b3, d3.

3.3.2 Leakage current due to corrosion for model fluxes under humidity exposure

Figure 7 shows the leakage current response of model flux activator contaminated SIR pattern under various climatic testing conditions. In general, leakage current value increased for all tested model flux residues with increasing RH for testing. Under the same testing condition, Fig. 7b1–b3 indicates that the thermal-activated adipic acid contained model fluxes contaminated SIR patterns exhibited the same leakage current values as no thermal activated sample

shown in Fig. 7a1–a3. High leakage current exceeding 10 µA occurred at 98% RH/60 °C for all five adipic acid model fluxes contaminated SIR patterns (shown in Fig. 7a3, b3). Figure 7a1–a3 demonstrates the amine additives did not influence the leakage current level of model fluxes with adipic acid activators under same testing condition. However, thermal activation significantly influenced the leakage current level of succinic acid contained model fluxes in different ways. Under testing temperature of 25 °C, thermal activated pure succinic acid induced high leakage current failure at 98% RH, whereas the leakage current level of none thermal activated pure succinic acid was below 1 µA. Under testing temperature of 40 °C, compared to the high leakage current failure of SIR pattern induced by all five non-thermal activated succinic acid fluxes shown in Fig. 7c2, thermal activation at 240 °C for amine modified succinic acid model fluxes suppressed the leakage current level SIR pattern under 98% RH exposure (Fig. 7d2).
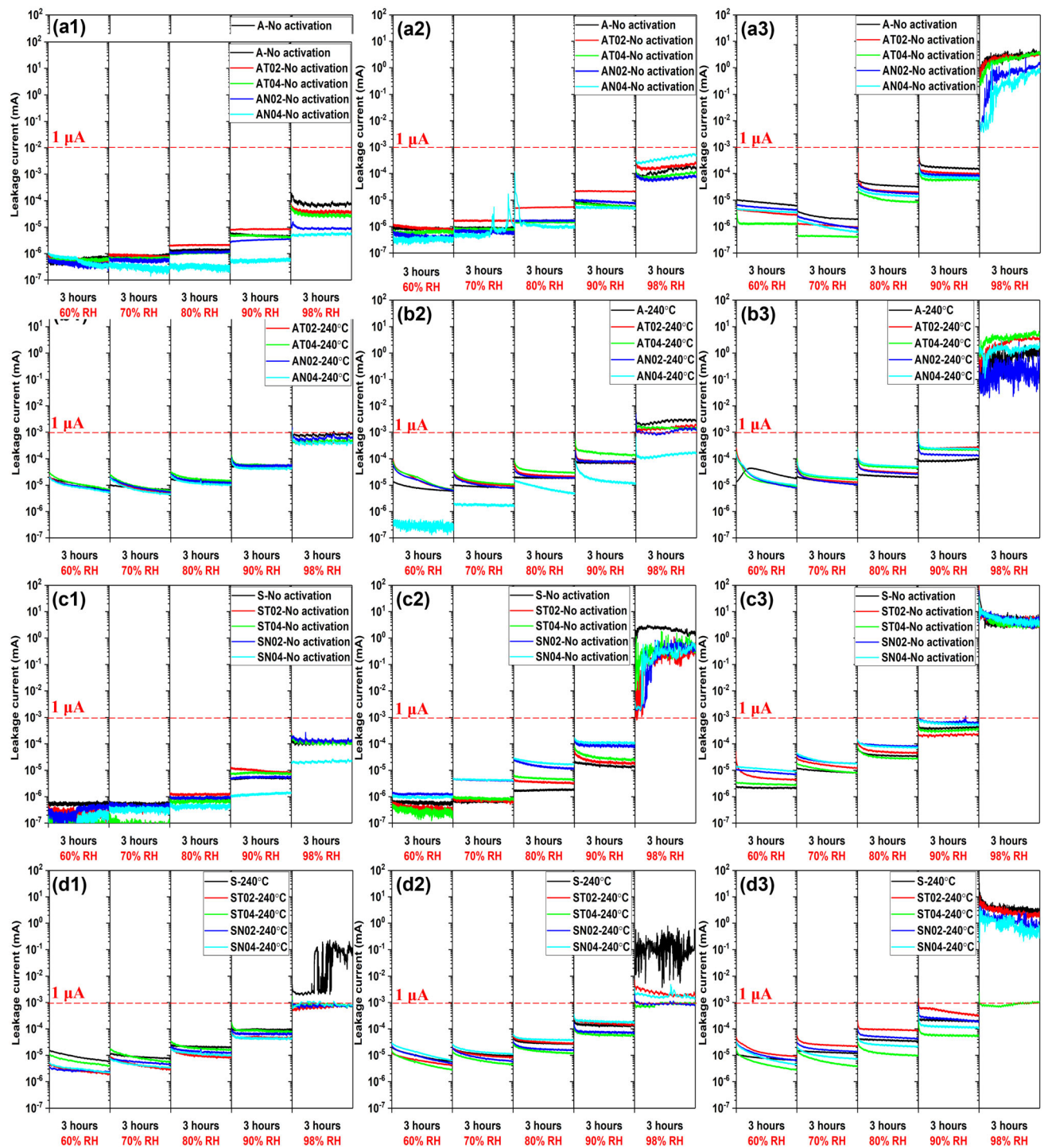
Fig. 7 Leakage current results of the model fluxes contaminated SIR pattern under various testing condition: **a** non-thermal activated adipic acid model fluxes, **b** 240 °C activated adipic acid model fluxes, **c** non-thermal activated succinic acid model fluxes, **d** 240 °C activated succinic acid model fluxes; under testing temperature of (1) 25 °C, (2) 40 °C, (3) 60 °C

4 Discussion

Present investigation demonstrates the effect of tripropylamine and naphthylamine additives on the solderability and corrosion reliability of commercial used WOA activator residue on PBA after simulated wave soldering condition, which summarized in Table 4.

The Cu oxide removal mechanism using WOA activators was achieved through the complexation (Eq. 1) and disproportionation (Eq. 2) reactions [37], where the R in carboxylic acid represents as an organic radical [4].

$$CuO + 2RCOOH = Cu(RCOO)_2 + H_2O, \qquad (1)$$

$$Cu_2O + 2RCOOH = Cu(RCOO)_2 + Cu + H_2O. \qquad (2)$$

The succinic acid with shorter organic carbon chain shows high polarity and lower pKa values in comparison with adipic acid, as shown in Table 1. From the solderability point view, result in Table 3 demonstrates that the succinic acid possessed higher maximum wetting force value compared to adipic acid. However, the higher ionization strength of succinic acid also lead to higher leakage current [18] and ECM failure [32] under humidity exposure with 10 V DC bias loading, while the leakage current value induced by adipic acid was located in the safety range below 1 μA under 25 °C and 40 °C [32]. Present study exhibited the improvement of the leakage current performance and the wetting speed of succinic acid model flux after addition of tripropylamine. On the other hand, after addition of 0.4 wt% tripropylamine in adipic acid model flux, the F_{max} and wetting speed of AT04 flux was improved in comparison with pure adipic acid and pure succinic acid model fluxes. At the same time, the leakage

current value of the tripropylamine additive modified adipic acid model fluxes maintained at safe level below 1 μA as pure adipic acid model flux, as shown in Fig. 7b1–b3.

4.1 Influence of amine additives in WOA model fluxes on the etching ability on copper surface

Tripropylamine and naphthylamine additives exhibit different influences on the wetting properties of adipic acid and succnic acid based fluxes. Reaction between WOA and amine can be consider as Brønsted–Lowry acid base reaction shown in Eq. 3, where R′ and R″ represent organic radicals.

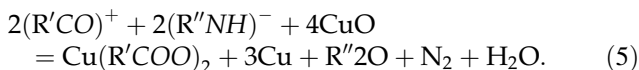$$R'COOH + R''NH_2 = R' - CO(NH) - R'' + H_2O. \qquad (3)$$
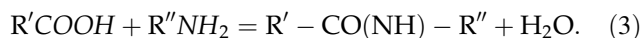
In the case of succinic acid based model fluxes, significant improvement of the wetting speed was obtained by the tripropylamine and naphthylamine modified flux formulation as shown in Table 3; however, the maximum wetting forces of all the amine modified fluxes did not exceed the pure succinic acid model flux. The wetting speed and F_{max} were influenced by the oxides removal mechanism of amine modified succinic acid based fluxes. Figure 5c, d demonstrates C=O stretching bond at 1725 cm^{-1} and C–N stretching bond at 1106 cm^{-1} for amide disappeared after simulated wave soldering process at 240 °C. The degradation of amide triggered the formation of the more reactive positive charge group $(R'CO)^+$ and negative charge group $(R''NH)^-$ at the initial thermal activation stage during soldering process as demonstration in Eq. 4. The oxides removal reaction between CuO and the degradation product of amide was demonstrated as Eq. 5. In

Table 4 Summary of solderability and leakage current performance for tested WOA activators with amine additives

Model flux	Solderability compared to WOA	Leakage current compared to WOA
AT02	Wetting force hignly inproved, wetting speed slightly reduced	No significant change
AT04	Wetting force highly improved, wetting speed slightly improved	No significant change
AN02	Wetting force highly improved, wetting speed highly reduced	No significant change
AN04	Wetting force slightly reduced, wetting speed highly reduced	No significant change
ST02	Wetting force highly improved, wetting speed highly improved	No ECM at 25 °C and 40 °C
ST04	Wetting force higly improved, wetting speed highly improved	No ECM at 25 °C and 40 °C
SN02	Wetting force slightly improved, wetting speed highly improved	No ECM at 25 °C and 40 °C
SN04	Wetting force slightly inproved, wetting speed highly improved	No ECM at 25 °C and 40 °C

comparison with relative higher T_0 and $T_{2/3}$ values obtained by pure succinic acid fluxes, the faster wetting speed of amine additive modified succinic fluxes could be due to the reaction between CuO and the more reactive $(R'CO)^+$ as well as $(R''NH)^-$ charge groups during soldering process. As a result, the localized spreading appearance was obtained using amine modified succinic acid fluxes, as shown in Fig. 2b2–5. After simulated soldering process, the shift of the carboxylic acid C=O stretching bond for ST04, SN02 and SN04 model fluxes in Fig. 5d indicates active carboxylic group of succinic acid was consumed by amine additives to form amide, which reduced the number of carboxylic group in participation of the oxide removal during soldering process. In consequence, the reduction of F_{max} was more pronounced for the 0.4 wt% amine additive modified succinic based model fluxes shown Table 3, and the thicker layer of SAC 305 alloy was observed on Cu substrate compared to pure succinic acid flux (Eq. 4b1, b3). Significant reduction of F_{max} was obtained by naththylamine modified succinic acid. This could be attributed to the covalent π bond of benzene ring in naphthylamine re-allocated the electron density in amide molecule, hence reduced the polarity of the carboxylic group. Therefore, the activation of the carboxylic group in the amide formed by naphthylamine and succinic acid was prohibited during soldering process, which triggered thicker layer of the SAC 305 alloy coated on the Cu substrate as shown in Eq. 4b4, b5.

$$R' - CO(NH) - R'' = (R'CO)^+ + (R''NH)^-, \qquad (4)$$

$$2(R'CO)^+ + 2(R''NH)^- + 4CuO \\ = Cu(R'COO)_2 + 3Cu + R''2O + N_2 + H_2O. \qquad (5)$$

However, amide bond was not detected in the flux formulation with amine additive and adipic acid, as shown in Fig. 5a. Therefore, the oxide removal reaction by adipic acid and amine additives were subjected in parallel during soldering process. Apart from the oxide removal process of by adipic acid, the increase of F_{max} for tripropylamine modified adipic acid based flux was attributed to the redox reaction between tripropylamine and CuO during soldering process, which is demonstrated in Eq. 6. As result, larger spreading area of the SAC 305 alloy was obtained by AT02 and AT04 in comparison with pure adipic acid flux, shown in Fig. 2a1–a3. Compared to tripropylamine modified adipic acid fluxes,

significant increase of T_0 and $T_{2/3}$ values was obtained using naphthylamine additive in adipic acid model fluxes, shown in Table 3. The covalent π bond in naphthylamine additive may prohibit the activity of carboxyl group in adipic acid, which required more energy and longer time for the complexation reaction to take palce between carboxylic groups in adipic acid and the oxides on the metal surface. In consequence, 0.4 wt% naphthylamine additive modified adipic acid flux (AN04) required longer time to reach to maximum wetting force in comparison with 0.2 wt% naphthylamine modified adipic acid flux (AN02). Therefore, the increasing trend of wetting force for AN04 was still visible at 10 s as shown in Fig. 3a.

$$3CuO + 2R''NH_2 = 2Cu + R_2O + N_2 + H_2O. \qquad (6)$$
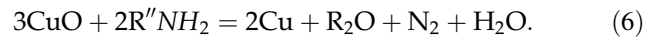
4.2 Influence of amine additives on the humidity interaction and leakage current response

Humidity interaction of the WOA activator residue on PBA was dependent upon the hygroscopicity of the WOA or its degradation products after soldering process, which triggered the moisture adsorption and absorption from the environment [18]. The hygroscopicity of the flux residue on SIR comb pattern was roughly estimated by single frequency EIS measurement in previous work [14, 32, 45]. Table 5 shows the DRH value of adipic acid and succinic acid from the literature under testing temperature of 25 °C, 40 °C and 60 °C respectively, which were comparable with the single frequency EIS measured DRH values for the tested WOAs in the present work. After water condensation triggered by WOA at lower RH value, the solubility of WOA and dissociation constant of carboxyl groups played the key role on the conductivity and corrosivity of the electrolyte formed on the surface of PBA. Under testing temperature of 25 °C, low solubility for adipic acid (0.17 mol/L) and succinic acid (0.69 mol/L) resulted in high impedance response of pure WOA contaminated SIR pattern under 99% RH exposure, as shown in Fig. 6a1, c1. As a consequence, low leakage current was observed due to less ionization of WOA on the surface of PBA (Fig. 7 a1, c1). When the testing temperature increased to 40 °C, the drop of impedance for pure succinic acid model flux contaminated SIR pattern shown in Fig. 6c2 was attributed to the much higher

Table 5 Summary of DRH values [32], and solubility [46] of tested WOA in literature with measured DRH in present work

Temperature	DRH in literature/measured DRH(% RH)			Solubility (mol/L)		
	25 °C	40 °C	60 °C	25 °C	40 °C	60 °C
Adipic acid	97.4/95	91.5/92	83.2/87	0.17	0.33	1.05
Succinic acid	94.2/98	91.3/95	82.2/88	0.69	1.16	2.22

solubility of 1.16 mol/L in comparison with 0.33 mol/L for adipic acid. As a result, the leakage current of succinic acid comtaminated SIR pattern exceeded 10 µA under 98% RH/40 °C (Fig. 7 a1), while the leakage current level of adipic acid contaminated SIR pattern remained at safety range (Fig. 7 c1). Solubility of adipic acid and succinic acid significantly increased under testing temperature 60 °C, which resulted the reduction of impedance (Fig. 6a3, c3) and high leakage current exceeding safety range (Fig. 7a3, c3). Since the WOA induced failures were more pronounced at high testing temperature and high RH, the influences of amine additives on the humidity interaction of WOA activators would be more representative under the testing temperature of 60 °C for adipic acid based flux, and above 40 °C for succinic acid based flux, as shown in Fig. 7b3, d3.

The role of the amine additives played in succinic acid based fluxes and adipic acid based fluxes were different, which resulted different performances of humidity interaction under testing temperature of 60 °C. FT-IR result in Fig. 5a shows the independent presence of the adipic acid and amine additive in flux residue. The ionization of the adipic acid and the protonation of amine additive simultaneously occurred in the condensed water. As result, intermolecular hydrogen bond formed by dipole–dipole interaction between carboxylic group and amino group [47] as shown in Eq. 7. The intermolecular hydrogen bond formed between adipic acid and amine additive could re-distribute the electron density of the polarized carboxyl group and amino group, which might reduce the polarity of adipic acid. Therefore, ERH of amine modified adipic acid flux shown in Fig. 6a3 significantly increased to 84% RH in comparison with 69% RH obtained by pure adipic acid at 60 °C. Moreover, the Van der Waals force of intermolecular hydrogen bond between adipic acid and amine additives might reduce the number of the free ions in the electrolyte. Therefore, the impedance response of amine modified adipic acid is much better than pure adipic acid as shown in

Fig. 6a3. While for succinic acid based model fluxes with amine additives, amide formation was confirmed by FT-IR analysis, as shown in Fig. 5c. Amide group appeared to be polar since oxygen and nitrogen can form hydrogen bond with water in atmosphere [48]. Therefore, minimal improvement of DRH and ERH was obtained by the amine additive modified succinic acid fluxes, as shown in Fig. 6c3.

$$R'COOH + R''NH_2 = R'COOH \cdots NH_2R'' \qquad (7)$$

Thermal activation played a vital role on the humidity robustness of the amine modified model fluxes. In the case of adipic acid based fluxes, the DRH and ERH value of tripropylamine additive modified fluxes increased from 90% RH and 84% RH to 95% RH and 95% RH after thermal activation, which might be attributed to the thermal degradation product of tripropylamine. However, the mechanism required further chemical analysis. In comparison, the soldering temperature of 240 °C is not able to evaporate or degrade naphthylamine due to its higher boiling temperature at 300.8 °C. As result, the DRH and ERH value of naphtylamine modified fluxes did not change after thermal activation. For the succinic acid based fluxes, significant improvement of ERH was obtained after thermal activation, which is due to the thermal degradation of the amide, as shown in Fig. 5d. The carboxylic acid C=O stretching peak at 1685 cm^{-1} shifted towards amide C=O stretching peak after thermal activation, which indicates the presence of limited amount of amide group in flux residue. After thermal activation, the 0.4 wt% tripropylamine modified succinic acid flux (ST04) obtained the largest shift C=O stretching peak, as shown in Fig. 5d. In consequence, moisture desorption behavior of ST04 is slightly worse compared to naphthylamine modified succinic acid fluxes (Fig. 6d3). Under 10 V DC bias loading, the degradation of amide reduced the polarity of the flux reside and coherently triggered the lower moisture absorption under testing condition of 98% RH/40 °C,

which lead to the significant reduction of the leakage current response shown in Fig. 7d2.

5 Conclusions

- FT-IR results indicate both tripropylamine and naphthylamine are able to form amides with succinic acids after flux formulation, while the adipic acid and amine additives did not. Thermal degradation of the amide C=O stretching bond was detected in the amine additive modified succinic acid based fluxes.
- Solderability testing showed improvement of the wetting speed using tripropylamine and naphthylamine additive in succinic acid based model fluxes; however, the maximum wetting force was reduced by tripropylamine and naphthylamine additive. The 0.2–0.4 wt% tripropylamine additive in adipic acid based model fluxes significantly increased the maximum wetting force.
- Single frequency EIS results show the tripropylamine and naphthylamine additives in adipic acid based model fluxes significantly increased the ERH and DRH in comparison with pure adipic acid flux under testing temperature of 60 °C. Thermal activation at 240 °C significantly increased ERH of two amine additives modified succinic acid based fluxes and adipic acid based fluxes.
- Leakage current testing results indicate the tripropylamine and naphthylamine additive in succinic acid model fluxes significantly decreased the leakage current level below threshold value of 1 μA under testing condition of 98% RH/25 °C and 98% RH/40 °C after simulated soldering process.
- Thermal degradation of the amide bond and amine additive under wave soldering temperature is able to improve the wetting speed during soldering process and enhance the life span from corrosion reliability point of view.

Author contributions

All the testing experiments were conducted by FL in Technical University of Denmark under supervision of Prof. RAt and Dr. MSJ.

Data availability

Can be provided when required.

Code availability

None.

Declarations

Conflict of interest The authors declare that they have no conflict of interest.

References

1. B.N. Ellis, Contamination control and the Montreal protocol. Circuit World **15**, 43 (1989)
2. S. Menon, E. George, M. Osterman, M. Pecht, High lead solder (over 85 %) solder in the electronics industry: RoHS exemptions and alternatives. J. Mater. Sci. Mater. Electron. **26**, 4021 (2015)
3. Z. Bukhari, K.C. Wong, Elimination of CFC's and the chemical waste with the use of no-clean solder in RF power module, in *Proc. 1996 IEEE Int. Symp. Electron. Environ. ISEE-1996* (1996), pp. 307–312
4. B.A. Smith, L.J. Turbini, Characterizing the weak organic acids used in low solids fluxes. J. Electron. Mater. **28**, 1299 (1999)
5. K.N. Subramanian, Lead-Free Electronic Solders: A Special Issue of the Journal of Materials Science: Materials in Electronics (2007)

6. E. Bastow, The Effect of Reflow Profiling on the Electrical Reliability of No-Clean Solder Paste Flux Residues, in *IPC APEX EXPO Proc.* (Las Vegas, 2014).

7. S. Wakeel, A.S.M.A. Haseeb, M.A. Amalina, K.L. Hoon, Investigation into chemistry and performance of no-clean flux in fine pitch flip-chip package. IEEE Trans. Components, Packag. Manuf. Technol. **12**, 155 (2022)

8. S. Wakeel, A.S.M.A. Haseeb, M.A. Afifi, S. Bingol, K.L. Hoon, Constituents and performance of no-clean flux for electronic solder. Microelectron. Reliab. **123**, 114177 (2021)

9. M. Wang, M. Yuan, C. Wang, R. Ma, Abietic acid encapsulated Sn-57Bi alloy nanoparticles as oxidation resistant solder material. Colloids Surf. A **602**, 125083 (2020)

10. S. Zhan, M.H. Azarian, M.G. Pecht, Surface insulation resistance of conformally coated printed circuit boards processed with no-clean flux. IEEE Trans. Electron. Packag. Manuf. **29**, 217 (2006)

11. A. Hanss, G. Elger, Residual free solder process for fluxless solder pastes. Solder. Surf. Mt. Technol. **30**, 118 (2020)

12. J.H. Lau and N.-C. Lee, in *Assem. Reliab. Lead-Free Solder Joints* (Springer, Singapore 2020), pp. 217–298.

13. W. Leske, J. Koch, Water-Rinsable or so-called 'No Clean' solder pastes? The attempt of a comparison from the technical and environmental viewpoint. Solder. Surf. Mt. Technol. **4**, 42 (1992)

14. K. Piotrowska, V. Verdingovas, R. Ambat, Humidity-related failures in electronics: effect of binary mixtures of weak organic acid activators. J. Mater. Sci. Mater. Electron. **29**, 17834 (2018)

15. B. Tolla, D. Jean, H. Bhavsar, Y. Shi, and X. Wei, Reactivity of no-clean flux residues in electronic assemblies: a systematic study, in *SMTA Int.* (Rosemont, IL, 2015).

16. K.-L. Lin, Y.-T. Liu, Manufacturing of solder bumps with Cu/Ta/Cu as under bump metallurgy. IEEE Trans. Adv. Packag. **22**, 580 (1999)

17. Y. Zhou, L.J. Turbini, D. Ramjattan, B. Christian, M. Pritzker, Characterizing corrosion effects of weak organic acids using a modified bono test. J. Electron. Mater. **42**, 3609 (2013)

18. V. Verdingovas, M.S. Jellesen, R. Ambat, Solder flux residues and humidity-related failures in electronics: relative effects of weak organic acids used in no-clean flux systems. J. Electron. Mater. **44**, 1116 (2015)

19. M.R. Harrison, J.H. Vincent, H.A.H. Steen, Lead-free reflow soldering for electronics assembly. Solder. Surf. Mt. Technol. **13**, 21 (2001)

20. J. Pan, B.J. Toleno, T.-C. Chou, J.D. Wesley, The effect of reflow profile on SnPb and SnAgCu solder joint shear strength. Solder. Surf. Mt. Technol. **18**, 48 (2006)

21. K.S. Hansen, M.S. Jellesen, P. Moller, P.J.S. Westermann, and R. Ambat, Effect of solder flux residues on corrosion of electronics. in *Annu. Reliab. Maintainab. Symp.* (2009), pp. 502–508.

22. H. Conseil, M.S. Jellesen, R. Ambat, Contamination profile on typical printed circuit board assemblies vs soldering process. Solder. Surf. Mt. Technol. **26**, 194 (2014)

23. P. Isaacs and T. Munson, What makes no-clean flux residue benign, in *2016 Pan Pacific Microelectron. Symp. (Pan Pacific)* (2016), pp. 1–7

24. S. Zhan, M.H. Azarian, M. Pecht, Reliability of printed circuit boards processed using no-clean flux technology in temperature-humidity-bias conditions. IEEE Trans. Device Mater. Reliab. **8**, 426 (2008)

25. V. Verdingovas, J.S. Joshy, M.S. Jellesen, R. Ambat, Circuit World **43**, 45 (2017)

26. P.-E. Tegehall, Impact of humidity and contamination on surface insulation resistance and electrochemical migration, in *ELFNET B. Fail. Mech. Test. Methods, Qual. Issues Lead-Free Solder Interconnects*, edited by G. Grossmann and C. Zardini (Springer, London, 2011), pp. 227–253

27. V. Verdingovas, M.S. Jellesen, R. Ambat, Influence of sodium chloride and weak organic acids (flux residues) on electrochemical migration of tin on surface mount chip components. Corros. Eng. Sci. Technol. **48**, 426 (2013)

28. S. Joshy, V. Verdingovas, M.S. Jellesen, R. Ambat, Circuit analysis to predict humidity related failures in electronics - Methodology and recommendations. Microelectron. Reliab. **93**, 81 (2019)

29. P. Isaacs, T. Munson, Cleanliness requirements: a moving target, in *2019 Pan Pacific Microelectron. Symp. (Pan Pacific)*, pp. 1–10 (2019)

30. D. Minzari, F.B. Grumsen, M.S. Jellesen, P. Møller, R. Ambat, Electrochemical migration of tin in electronics and microstructure of the dendrites. Corros. Sci. **53**, 1659 (2011)

31. X. Zhong, L. Chen, Z. Zhang, S. Gao, Electrochemical migration of Sn and Sn solder alloys: a review. RSC Adv. Soc. Chem. **7**, 28186 (2017)

32. K. Piotrowska, R.U. Din, F.B. Grumsen, M.S. Jellesen, R. Ambat, Parametric study of solder flux hygroscopicity: impact of weak organic acids on water layer formation and corrosion of electronics. J. Electron. Mater. **47**, 4190 (2018)

33. K. Piotrowska, R. Ambat, Residue-assisted water layer build-up under transient climatic conditions and failure occurrences in electronics. IEEE Trans. Components, Packag. Manuf. Technol. **10**, 1617 (2020)

34. D. Minzari, M.S. Jellesen, P. Møller, R. Ambat, On the electrochemical migration mechanism of tin in electronics. Corros. Sci. **53**, 3366 (2011)

35. V. Verdingovas, M.S. Jellesen, R. Ambat, Relative effect of solder flux chemistry on the humidity related failures in electronics. Solder. Surf. Mt. Technol. **27**, 146 (2015)

36 F. Li, K. Piotrowska, M.S. Jellesen, R. Ambat, Alkanolamines as activators in no-clean flux systems: investigation of humidity robustness and solderability. J. Mater. Sci. Mater. Electron. **32**, 4961–4981 (2021)

37. M. Bixenman, D. Lober, A. Ailworth, K. Corporation, B. Tolla, D. Ph, J. Allen, D. Jean, and K. Loomis, Electrochemical methods to measure the corrosion potential of flux residues, in *IPC APEX EXPO* (SMTNET, San Diego 2017)

38. D. Xu, X. Li, C. Wang, and B. Xu, Study on wettability and corrosivity of a new no-clean flux for lead-free solder paste in electronic packaging technology, in *2011 Second Int. Conf. Mech. Autom. Control Eng.* (2011), pp. 1706–1708

39. Y. Shi, X. Wei, and B. Tolla, The role of organic amines in soldering materials, in *IPC APEX EXPO Conf. Proc.* (Circuit Insight, San Diego, 2015).

40. G. Wable, Q. Chu, P. Damodaran, K. Srihari, Wave soldering using Sn/30Ag/05Cu solder and water soluble VOC-Free Flux. IEEE Trans. Electron. Packag. Manuf. **29**, 202 (2006)

41. R.P. Prasad, Soldering of Surface Mounted Components, in *Surf. Mt. Technol. Princ. Pract.* (Springer, Boston, 1997), pp. 533–597.

42. M. Hasnine, B. Tolla, M. Karasawa, Effect of Ge addition on wettability, copper dissolution, microstructural and mechanical behavior of SnCu–Ge solder alloy. J. Mater. Sci. Mater. Electron. **28**, 16106 (2017)

43. L. D'Angelo, V. Verdingovas, L. Ferrero, E. Bolzacchini, R. Ambat, On the effects of atmospheric particles contamination and humidity on tin corrosion. IEEE Trans. Device Mater. Reliab. **17**, 746 (2017)

44. S. Lauser, T. Richter, V. Vadimas, R. Ambat, Electrochemical Impedance Spectroscopy (EIS) for Monitoring the Water Load on PCBAs Under Cycling Condensing Conditions to Predict Electrochemical Migration Under DC Loads, in *2019 IEEE 69th Electron. Components Technol. Conf.* (2019), pp. 515–521

45. K. Piotrowska, M. Grzelak, R. Ambat, No-clean solder flux chemistry and temperature effects on humidity-related reliability of electronics. J. Electron. Mater. **48**, 1207 (2019)

46. A. Apelblat, E. Manzurola, Solubility of oxalic, malonic, succinic, adipic, maleic, malic, citric, and tartaric acids in water from 278.15 to 338.15 K. J. Chem. Thermodyn. **19**, 317 (1987)

47. Y.K. Hong, W.H. Hong, D.H. Han, Application of reactive extraction to recovery of carboxylic acids. Biotechnol. Bioprocess Eng. **6**, 386 (2001)

48. O.D. Bonner, S.C. Young, Water—amide interaction. Spectrochim. Acta Part A **31**, 1975 (1975)